Mode adaptive control of a kilowatt-level large mode area fiber laser based on 5×1 photonic lantern

Wenguang Liu [1,2,3,†], Yanyang Hu [1,2,3,†], Hanwei Zhang [1,2,3], Lianchuang Ding [1,2,3], Pengfei Liu [1,2,3], Baozhu Yan [1,2,3], Jiangbin Zhang [1,2,3], Qiong Zhou [1,2,3] and Zongfu Jiang [1,2,3]

[1] *College of Advanced Interdisciplinary Studies, National University of Defense Technology, Changsha 410073, China*

[2] *Nanhu Laser Laboratory, National University of Defense Technology, Changsha 410073, China*

[3] *Hunan Provincial Key Laboratory of High Energy Laser Technology, Changsha 410073, China*

Abstract This study presents high-power mode-selective operation in a large-mode-area (LMA) fiber laser. A spatial mode-adaptive control system incorporating a 5×1 photonic lantern was employed to facilitate mode conversion between the LP_{01} and LP_{11} modes. The coherence length between the five single-mode arms and the stimulated Brillouin scattering (SBS) threshold in the amplifier were well balanced by tuning the seed linewidth. Additionally, the specific design of the fiber amplifier's bending radius enabled stable mode-selective output with high mode purity. Consequently, a near-fundamental mode control was achieved in a 42-μm LMA fiber laser, yielding a beam quality M^2 factor of 1.97 at an output power of 1 kW. Subsequently, a stable LP_{11} mode laser output with an output power of 219 W and an optical conversion efficiency of 75% was obtained. This

This peer-reviewed article has been accepted for publication but not yet copyedited or typeset, and so may be subject to change during the production process. The article is considered published and may be cited using its DOI.

10.1017/hpl.2025.10059

research provides a significant technical foundation for the mode-selective operation of high-power LMA fiber lasers.

Key words: fiber amplifier, large-mode-area fiber, adaptive optics, photonic lantern

Correspondence to: College of Advanced Interdisciplinary Studies, National University of Defense Technology, Changsha 410073, China. Email: zhanghanwei100@163.com (Hanwei Zhang) and ceastbons@163.com (Yanyang Hu)
†These authors contributed equally to this work.

I. Introduction

Fiber lasers have garnered significant attention for the wide application in industrial manufacturing, defense, and scientific research [1-6]. However, scaling up the power of fiber lasers while maintaining near-diffraction-limited beam quality remains a major challenge due to nonlinear effects, such as Stimulated Brillouin Scattering (SBS) and Stimulated Raman Scattering (SRS) [7-9]. Large-mode-area (LMA) fiber lasers offer a potential solution by enhance the SBS and SRS thresholds through reduced laser intensity in the core. Nevertheless, larger core size introduces dynamic mode coupling between the fundamental mode (FM) and higher-order modes (HOMs). The increase in modal contents degrades the beam quality [10-13], posing a significant challenge for LMA fiber lasers to maintain FM operation [14-16].

The photonic lantern (PL) has emerged as a promising solution for mode control in LMA fiber lasers, providing a new technical approach to achieve high output power with a FM [17-21]. In 2017, Lincoln Laboratory demonstrated adaptive mode control using a 3×1 photonic lantern, achieving a pump-limited 1.27 kW output power in a 25/400 μm gain fiber amplifier

https://doi.org/10.1017/hpl.2025.10059 Published online by Cambridge University Press

[22]. This technology holds potential for further mode control of high-power fiber lasers with larger core size. However, the team of MIT concluded that the number of input ports of PLs must equal to the number of the mode in the fiber amplifier. Therefore, based on this inference, we can anticipate that when employing a photonic lantern to achieve mode control in a LMA fiber with a 42-μm core diameter, where the number of modes will increase to 20 (with a NA of 0.069), the input ports of the photonic lantern will significantly increase, rendering the control system highly complex and costly [23]. Therefore, how to achieve effective mode control in LMA fibers using the minimum number of control ports has become a significant technical challenge for the practical application. Subsequent research by our group has found that the mode control of LMA fibers can be realized with fewer control ports. In 2024, Ze et al. experimentally demonstrated mode control in 42/400 fiber laser with a 3×1 photonic lantern [24]. However, the SBS and thermal lenses limits the power scaling. Meanwhile, as the core size increases, there is a significant rise in the number of HOMs, the M^2 factor of 2.2 was achieved in Ze's work. It shows that there are considerable challenges to realize high power and near FM output with fewer control ports of PLs.

In this work, we achieved enhanced control results over the HOMs of LMA at kilowatt-level output power with the combination of active and passive control method. The 5×1 photonic lantern possesses greater control capability for HOMs, and bending of fiber amplifier enables effective filter out of HOMs in 42 μm gain fibers. The coherence length and SBS threshold were well balanced by optimizing the linewidth of the seed source. In the experiment, the M^2 factor of 1.97 at an output power of 1kW is achieved. Further power scaling was pump-limited in 1 kW-level. We also achieved the control of LP_{11} with an output power of 219 W, and verified the

https://doi.org/10.1017/hpl.2025.10059 Published online by Cambridge University Press

possibility of HOMs operation by mode control technology. This study provides a technical basis for further research on mode adaptive control of higher-power fiber lasers with fewer ports PLs.

II. Principle of mode control with PL

The photonic lantern is an all-fiber passive optical device that connects a bundle of single-mode fibers (SMFs) and a multi-mode fiber (MMF) [25]. The structure of the 5×1 photonic lantern is shown in Fig. 1. As the number of photonic lantern input ports increases, the complexity of fabrication correspondingly escalates. In order to optimize the mode evolution process of photonic lantern, it is necessary to strictly control two structural parameters. The first is the lateral dimension, the cladding of SMFs is required to corrode from 10/125 μm to 10/90 μm, and the inner diameter of the low index capillary tube is reduced to 30 μm with the double tapering process. The second is the longitudinal dimension, the long taper region (20-mm) of the 5×1 photonic lantern facilitates highly efficient mode evolution.

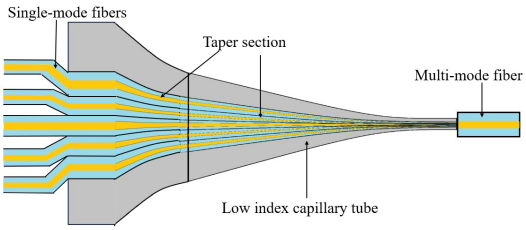

Fig.1. The structure of 5×1 photonic lantern using the double tapering method.

The unique structural of the photonic lanterns enables a mode-selective operation. The photonic lantern can be effectively approximated as an optical linear converter that facilitates the transition between FM and HOMs. This conversion process can be mathematically represented using a transmission matrix. The relationship between the input and output ports of the photonic lantern is expressed as: $Av = u$, where $v^T = \left[v_1 e^{j\theta_1}, v_2 e^{j\theta 2}, \cdots, v_i e^{j\theta i}\right]$ is the column vector describing the optical field of the SMFs (v_i, θ_i represents the amplitude and phase of the *i*-th input ports,

https://doi.org/10.1017/hpl.2025.10059 Published online by Cambridge University Press

respectively), and $u^T = \left[u_1 e^{j\theta_1}, u_2 e^{j\theta_2}, \cdots, u_n e^{j\theta n}\right]$ is the column vector describing the optical field of the MMF (u_n , θ_n represents the amplitude and phase of the LP_{nm} mode respectively). A is the transmission matrix of the photonic lantern.

$$A = \begin{bmatrix} 0.4e^{i\cdot(0\pi)} & 0.4e^{i\cdot(0\pi)} & 0.4e^{i\cdot(0\pi)} & 0.4e^{i\cdot(0\pi)} & 0.4e^{i\cdot(0\pi)} \\ 0.6e^{i\cdot(-0.3\pi)} & 0.2e^{i\cdot(-0.3\pi)} & 0.2e^{i\cdot(-0.3\pi)} & 0.5e^{i\cdot(0.7\pi)} & 0.5e^{i\cdot(0.7\pi)} \\ 0 & 0.5e^{i\cdot(-0.3\pi)} & 0.5e^{i\cdot(0.7\pi)} & 0.3e^{i\cdot(-0.3\pi)} & 0.3e^{i\cdot(0.7\pi)} \\ 0.25e^{i\cdot(-0.2\pi)} & 0.2e^{i\cdot(0.8\pi)} & 0.2e^{i\cdot(0.8\pi)} & 0.1e^{i\cdot(-0.2\pi)} & 0.1e^{i\cdot(-0.2\pi)} \\ 0 & 0.3e^{i\cdot(-0.2\pi)} & 0.3e^{i\cdot(0.8\pi)} & 0.5e^{i\cdot(0.8\pi)} & 0.5e^{i\cdot(-0.2\pi)} \end{bmatrix}$$

The specific modes (LP_{01}, LP_{11e}, LP_{11o}, LP_{21e} and LP_{21o} modes) can be selective generated by adjusting specific amplitudes and phases of the input ports. For example, when input ports are setting the same amplitudes and phases, $v^T = \left[0.4e^{i\cdot(0\pi)}, 0.4e^{i\cdot(0\pi)}, 0.4e^{i\cdot(0\pi)}, 0.4e^{i\cdot(0\pi)}, 0.4ie^{i\cdot(0\pi)}\right]$. The high pure LP_{01} mode is obtained in the output port. When the input ports information with specific amplitudes and phase are applied respectively, $v^T = \left[0.6e^{i\cdot(-0.3\pi)}, 0.2e^{i\cdot(-0.3\pi)}, 0.2e^{i\cdot(-0.3\pi)}, 0.5e^{i\cdot(0.7\pi)}, 0.5e^{i\cdot(0.7\pi)}\right]$. Those beam with the same phase will undergo a specific coupling process to enhance the LP_{11} mode[26, 27].

The evolution process of beam in the photonic lantern is numerically simulated based on beam propagation method (BPM) algorithm. Figure 2 shows that, the different input ports energy coupling occurs along the direction of propagation in different cross sections (A-E). After entering the waist region, the light evolves into a corresponding supermode, and then it is transferred into the output port. As an example, we monitor the content of LP_{01} and LP_{11} mode through the 5×1 photonic lantern structure. Figure 3(a) shows the content of LP_{01} mode of SMFs gradually decreases along the long taper region, and steadily maintain at 92% in the MMF. When the LP_{11} mode is regarded as the control target. As shown in Fig. 3(b), the content change of the

https://doi.org/10.1017/hpl.2025.10059 Published online by Cambridge University Press

LP_{01} mode presents a similar situation in the taper region. Finally, the content of LP_{11} mode is stable at about 88%.

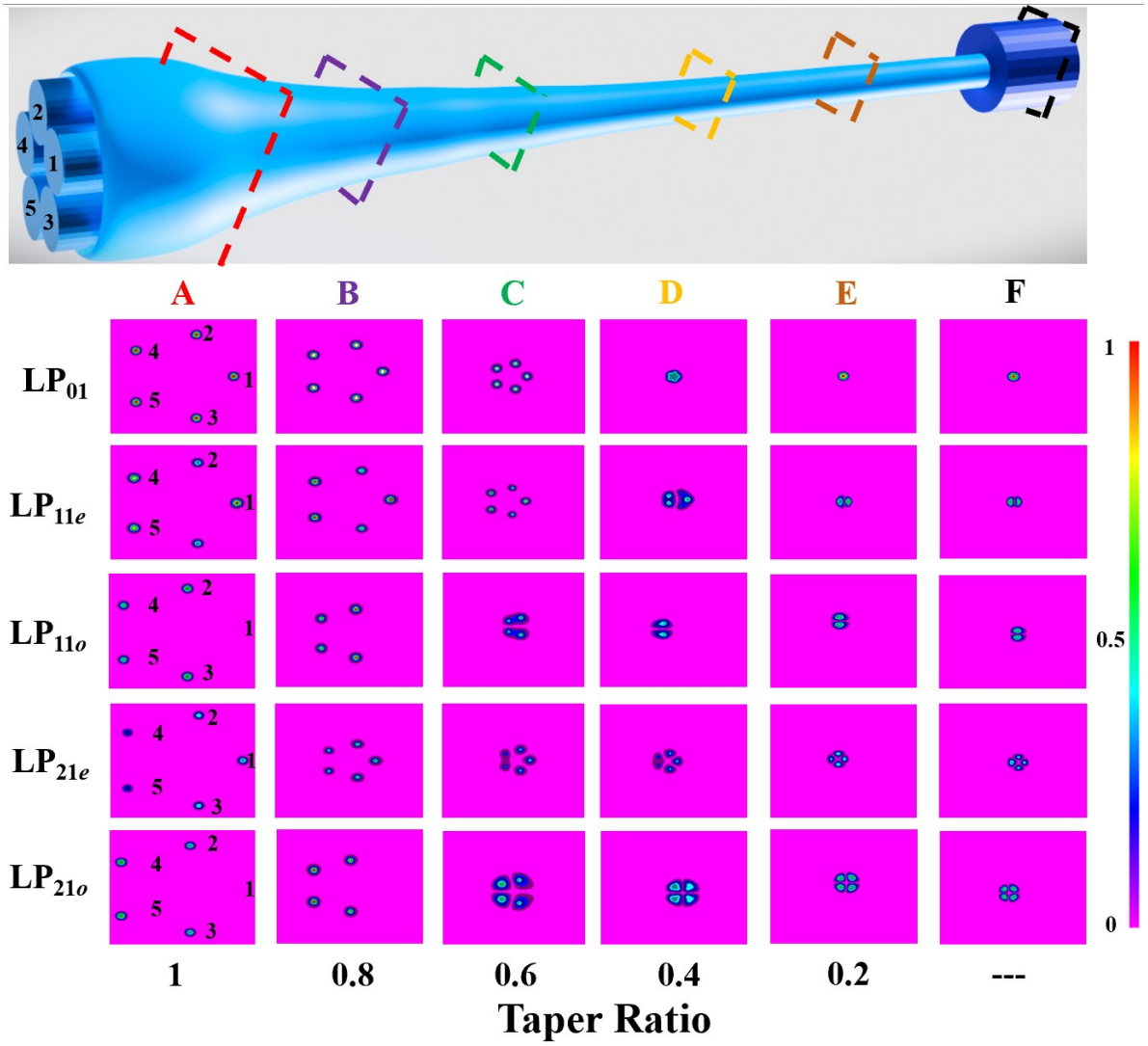

Fig.2. The mode evolution of the 5×1 photonic lantern varies with the taper ratio.

https://doi.org/10.1017/hpl.2025.10059 Published online by Cambridge University Press

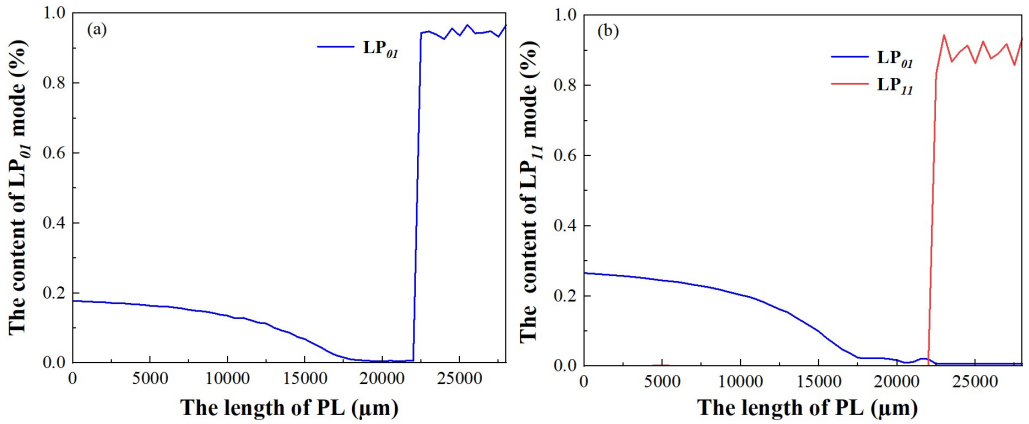

Fig. 3. The modal content evolution process in the 5×1 photonic lantern varies with the length of taper region. (a) Targeting the LP_{01} mode output. (b) Targeting the LP_{11} mode output.

III. Experimental setup

Experimental setup of the mode adaptive control system is shown in Fig. 4. The seed is a single-frequency laser operating at a wavelength of 1064 nm. The white noise source (WNS), driven by the radio frequency high-voltage amplifier, applies electrical signals to a $LiNbO_3$ electro-optic modulator (EOM), thereby achieving spectrum broadening to enhance the SBS threshold. The splitter can divide light into equal five parts. The phase of input SMFs are controlled by the phase modulators (PMs). The delay lines (DLs) are used to match optical path difference (OPD) of each input port. The isolators (ISOs) are fusion spliced with band-pass filterings (BPFs), this setup simultaneously filters out background spectral noise and isolates the reverse power.

The amplification system adopts two-stage amplification technology. In the preamplifiers systems, the output beam of the photonic lantern serves as the seed for the amplifier. The 976 nm laser diodes (LDs) are combined to pump 30/250 μm gain fiber (NA~0.066) via a (6+1) ×1 pump and signal combiner, and achieve a total output power of 40 W. The 915nm and 981nm semiconductor lasers are used to precisely control the pump absorption coefficient. The absorption coefficient of the gain fiber for pump light can be adjusted by combining 915nm and

https://doi.org/10.1017/hpl.2025.10059 Published online by Cambridge University Press

981nm pumping, which allows the thermal load per meter of the gain fiber to be controlled within a suitable range. Therefore, the fiber length is also controlled within a suitable range, which allows for simultaneous suppression of TMI and SBS effects at a kW-level output power [28]. The main amplifier consists of an 42/250 Yb-doped fiber (NA~0.069) and a (6+1) ×1 signal-pump combiner. Finally, a quartz block holder (QBH) embedded with cladding power strippers (CPS) is fused for simultaneously filtering excess pump light and outputting the beam.

The beam is received by a M^2 analyzer and a CCD for the purpose of beam quality evaluation. The power-in-the-bucket (PIB) detected by a photonic detector (PD) is used as the evaluation function of the stochastic parallel gradient descent (SPGD) algorithm. By measuring the corresponding change in intensity at the source, an approximate gradient with respect to the phase of each element can be calculated. The controller has an execution speed of more than 500 thousand times per second. Thus, the phase-locked loop can convergence can be completed within less than 100 iterations [29].

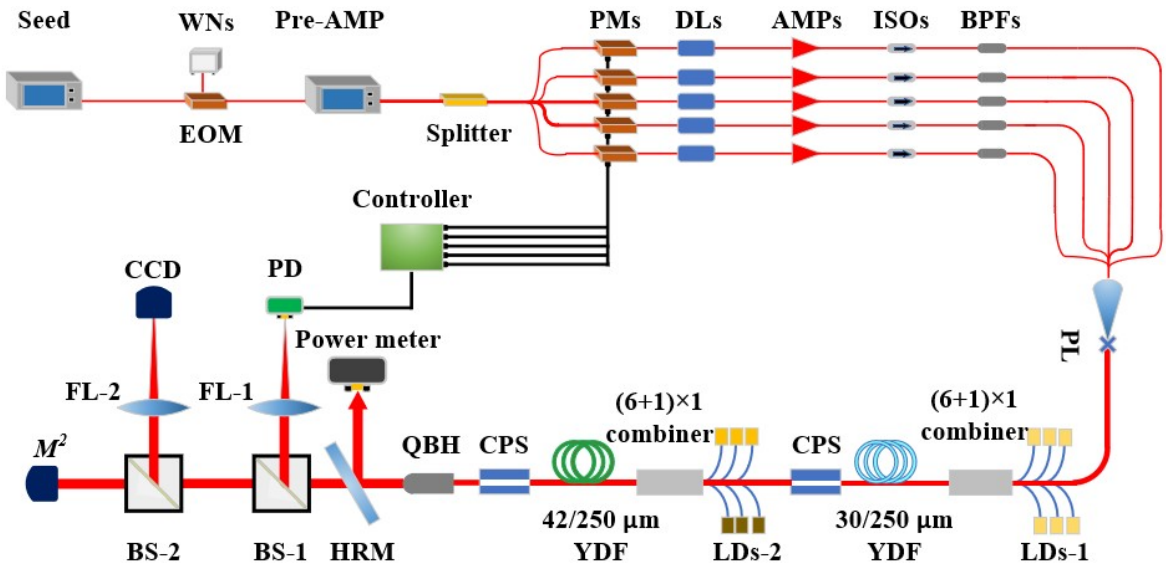

Fig. 4. The mode adaptive control system based on 5×1 photonic lantern.

When the laser system operates at high power, the LMA active fiber inevitably excited excessive more HOMs. For gain fiber with a core diameter of 42 μm, over twenty modes can be

https://doi.org/10.1017/hpl.2025.10059 Published online by Cambridge University Press

supported. We employed the method of bending the fiber to reduce the number of modes in the LMA fibers[30]. The FM and HOMs loss with respect to the bending radius are illustrated in Fig. 5. As the bending radius decreases, the bend loss of both the FM and HOMs increases nonlinearly. Notably, the higher-order mode shows a stronger sensitivity to the physical deformation of fiber bending, and its bending loss demonstrates a more pronounced increasing trend compared to lower-order modes. Controlling the bending radius of LMA fibers serves dual objectives. Firstly, the bend loss of LP_{01}, LP_{11e}, LP_{11o}, LP_{21e} and LP_{21o} modes maintain low loss level, thereby enabling highly efficient and high-purity signal transmission. Secondly, other higher-order modes losses are large enough to have more efficient mode control of the photonic lanterns. As depicted in Fig. 5, when the bending radius is 7 cm, the bending loss for the LP_{21} modes amount to 0.02 dB/m while that of LP_{02} mode reaches 1.36 dB/m. In the experiment, we choose the bending radius of 7 cm, ensuring that only LP_{01}, LP_{11e}, LP_{11o}, LP_{21e} and LP_{21o} modes can be transmitted in the gain fiber. This approach of employing fiber bending to reduce the number of modes not only reduce modes crosstalk but also enables more precise controlling of the target mode.

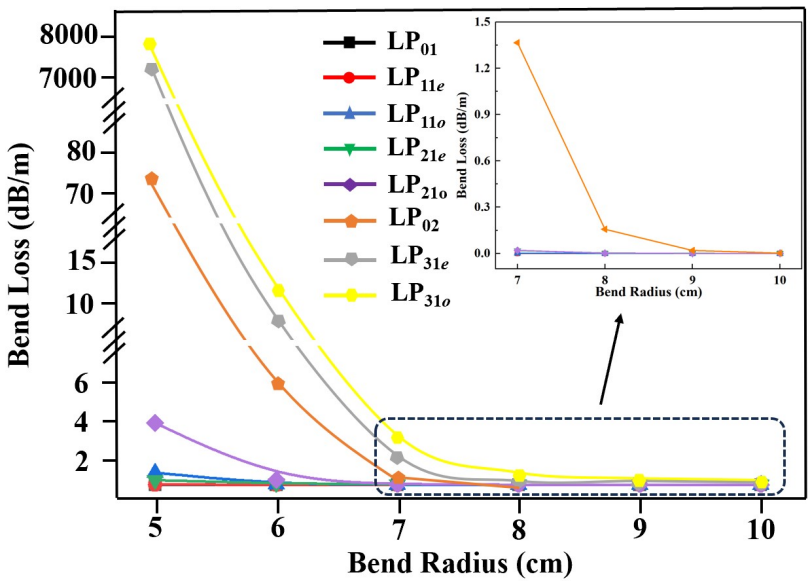

Fig. 5. Bend loss of different modes versus bend radius.

https://doi.org/10.1017/hpl.2025.10059 Published online by Cambridge University Press

For the high-power mode adaptive control system, the requirements of high SBS threshold and high coherence of the input ports must be met simultaneously. In order to improve the coherence of each input port, it is essential to utilize a seed laser with narrower spectrum width. However, the reduction in the spectrum linewidth leads to decrease of the SBS threshold, which consequently limits the ability to amplify the output power. Figure 6 shows the SBS threshold of the fiber amplifier within mode control adaptive systems measured at various spectra width. When the output power exceeds the SBS threshold, a pronounced Stokes peak emerges in the spectrum as shown in Fig. 6(a). The SBS threshold conversion with the spectra width is shown in Fig. 6(b). As the spectra width rises, the SBS threshold exhibits a nonlinear increase. Until the SBS threshold exceeds 1 kW with the spectrum width of 18 GHz.

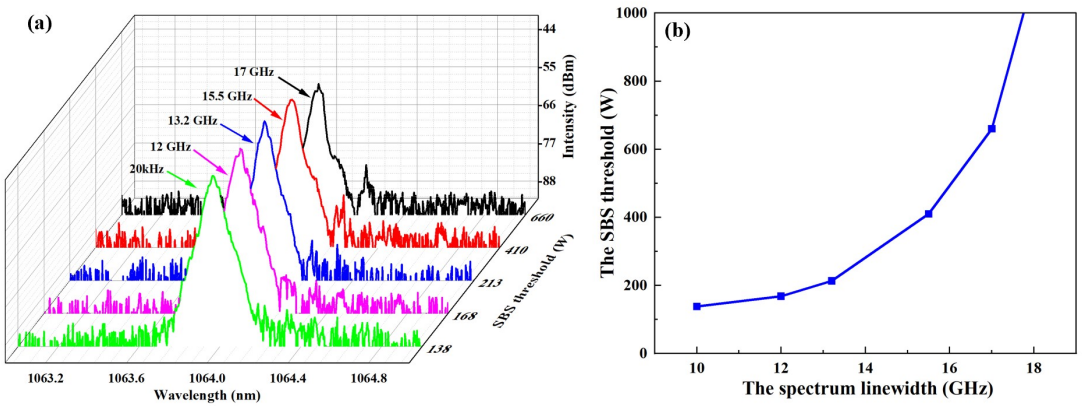

Fig. 6. Comparison of the SBS threshold of different 3 dB linewidth. (a) The spectrum of the SBS effect is occurring with the different spectra width. (b) The SBS threshold versus the spectra width.

However, the corresponding coherence length of each input port are only 16 mm with the spectrum width of 18GHz. To ensure the optical lengths of each input port are precisely confined within the coherence length, it is necessary to employ high-precision optical metrology technique to measure the fiber length. We utilized a picosecond pulsed laser source (the repetition frequency of 9 MHz, the pulse width of 1 ns) to measure the OPD of each input port, as shown in Fig. 7(a). By analyzing the pulse time delays on the oscilloscope, the differences in the fiber

https://doi.org/10.1017/hpl.2025.10059 Published online by Cambridge University Press

length between the input ports can be measured. Before compensation, Figure 7(b) shows that the minimum OPD is 259 ps, corresponding the fiber length difference of 5.38 cm. Based on the results, we trimmed the fiber length of each input port, ultimately controlling the OPD within 20 ps, corresponding the fiber length difference of 4.3 mm, as shown in Fig. 7(c). This value falls within the adjustable range of the DLs, ensuring precise phase matching and optimal system performance.

Through the implementation of fiber bending, spectral linewidth optimization, and optical path difference adjustment, we demonstrate a mode adaptive control system based on 5×1 photonic lantern, which enable effective mode control and power scaling in 42 μm LMA fiber lasers with a minimized number of control ports.

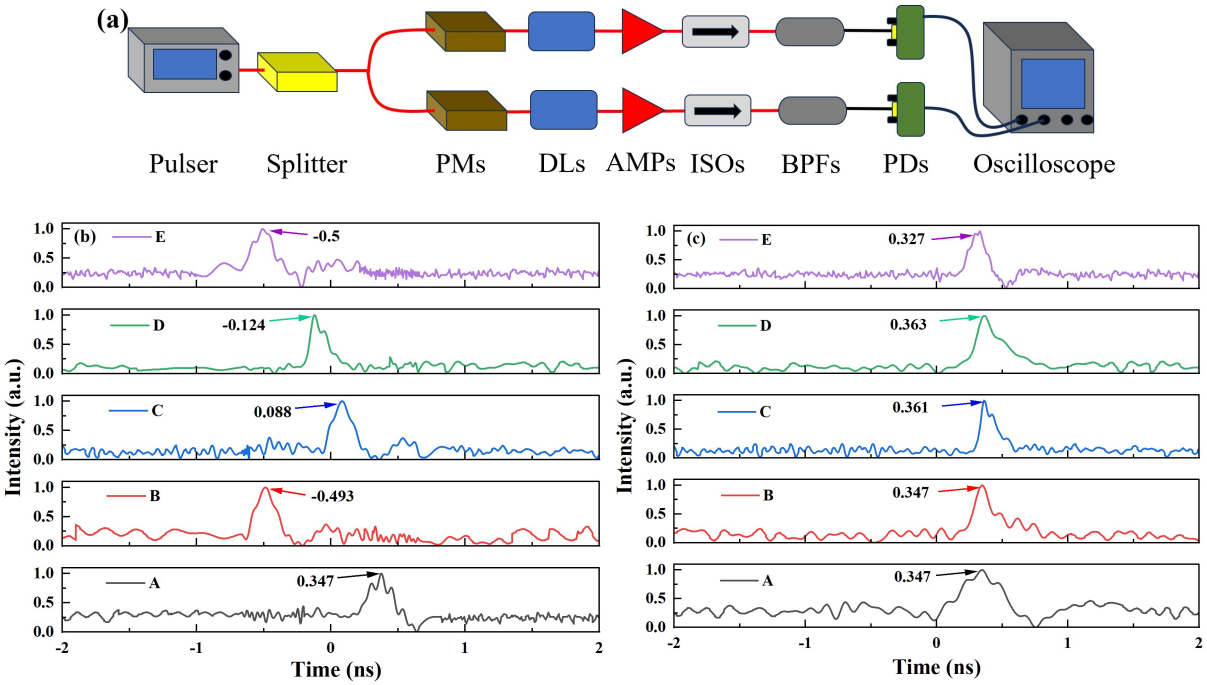

Fig. 7. The results of measuring and compensating the OPD. (a) Experimental setup for measuring OPD of the photonic lantern. (b) The OPD among five input ports fibers of the photonic lantern before compensation, and (c) after compensation.

IV. Results and discussion

https://doi.org/10.1017/hpl.2025.10059 Published online by Cambridge University Press

When the FM is designated as the control target mode, the output characteristics of the fiber amplifier based on photonic lantern are investigated first. The output power conversion with the pump power is shown in Fig. 8(a). As the pump power rises, the output power exhibits a linear and stable increase. Finally, more than 1 kW output power is achieved with an optical conversion efficiency of 73%. For conventional fiber lasers, further power amplification may be limited by SBS and TMI. However, in a photonic-lantern-based fiber laser, the SBS threshold in the amplifier can be well suppressed by tuning the seed linewidth and the optical path of input ports. Meanwhile, the high frequency disturbance in photonic lantern will setup a fast refreshed multimode interference optical field to disrupt the thermally-induced refractive index in the gain fiber. So, the photonic-lantern-based fiber laser will suppress the TMI well in LMA fiber. As shown in Fig. 8(b), a pure output spectrum without nonlinear characteristic peaks is presented with the different output power. Meanwhile, the detailed spectra of the signal laser at different pump powers are also measured as shown in Fig. 8(c).

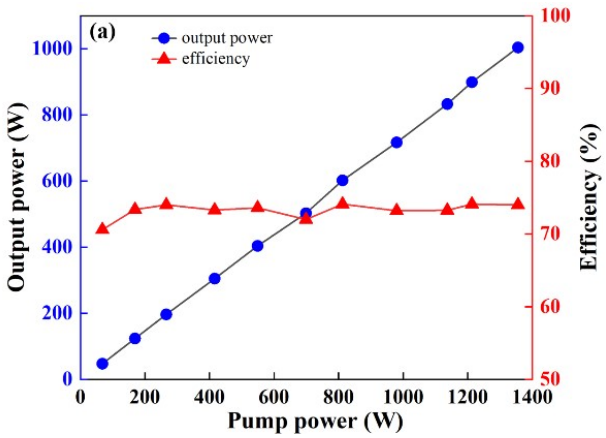

https://doi.org/10.1017/hpl.2025.10059 Published online by Cambridge University Press

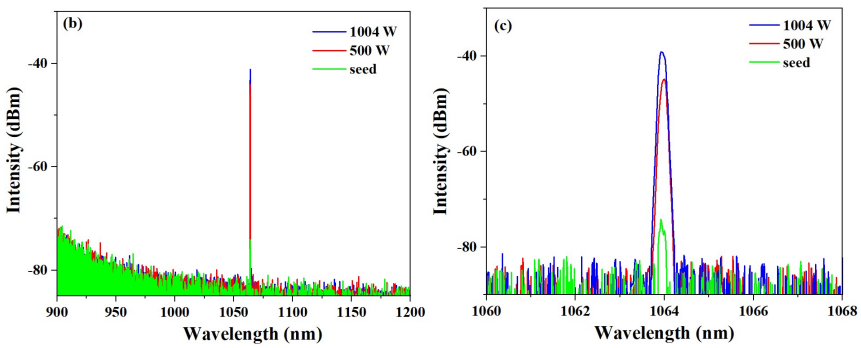

Fig. 8. Output properties of the fiber amplifier based on the 5×1 photonic lantern. (a) Output power and efficiency versus pump power. (b) Spectra at different output power. (c) The detailed spectra at different output power.

The SPGD algorithm adaptively controls the phase of the input ports fiber, by utilizing max PIB as the evaluation function. At the maximum output power, the on-axis signal of the PD changing over time is shown in Fig. 9(a). Before the control is turned on, the output field is generally a superposition of the FM and the HOMs, and the voltage signal exhibits significant fluctuations. After the control is turned on, a stable high-level signal is received by the PD. Figure 9(b) shows the beam quality and the content of LP_{01} mode of the output laser versus the output power. The M^2 factor of the seed laser is 1.28, after passing through the pre-amplification it is reduced to 1.47. Then at the highest output power of 1007 W, the M^2 factor is 1.97. As the pump power increases, the modal content of LP_{01} mode attenuates from 96 % to 86%. The complete mode decomposition effect is evaluated by numerical method [31]. The mode decomposition results are shown in the Fig. 9(c). The modal content of the LP_{01} mode is 86.46 % with the output power of 1kW. The correlation coefficient between the measured spot and the reconstructed spot is 0.9906. Furthermore, the system demonstrates the capability to generate HOMs. When the target mode is set to LP_{11} mode, the output characteristics of the fiber amplifier is shown in Fig. 9(d). The LP_{11} mode output was achieved at the output power of 219 W with a high optical conversion efficiency of 75%. However, this system creates more intense

https://doi.org/10.1017/hpl.2025.10059 Published online by Cambridge University Press

mode competition after the amplifier, and then the LP_{11} modal content caused a drop from 90 % to 75 %.

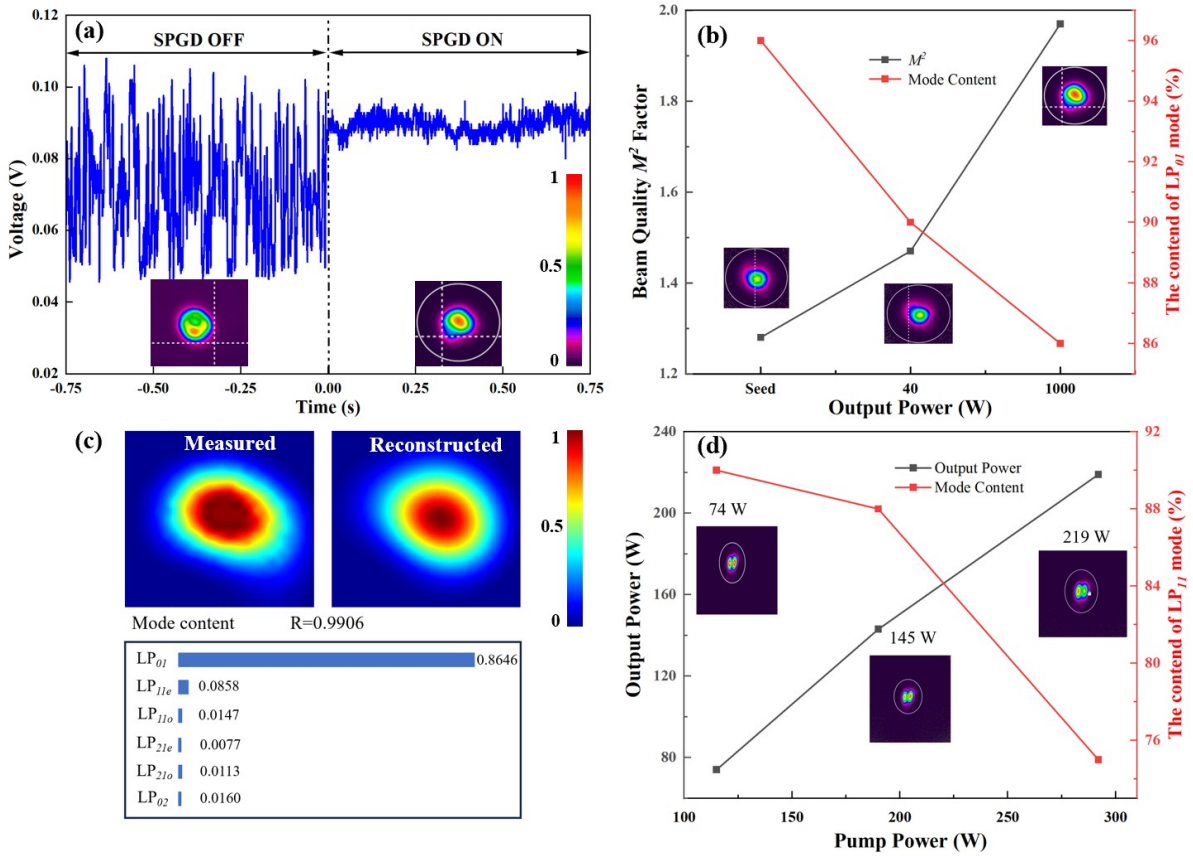

Fig. 9. The beam profiles of the 5×1 photonic lantern amplifier. (a) The PD signal over time when SPGD was turned off and on. (b) Beam quality and mode content versus the LP_{01} output power. (c) Mode decomposition of the obtained beam. (d) Output power and mode content of LP_{11} mode versus the pump power (insets: beam profiles).

https://doi.org/10.1017/hpl.2025.10059 Published online by Cambridge University Press

Table 1 Output performances of mode-selective operation in fiber laser with different method

Method	Gain fiber	Output power of LP_{01} mode	Output power of LP_{11} mode	Ref
Long-period grating	25/250	117 W	117 W	[3]
Long-period grating	25/250	56.79 W	54.51 W	[32]
Fiber squeezer	20/400	500 W	500 W	[33]
Fiber squeezer	25/400	1389 W	1396 W	[34]
Photonic lantern	13/163	90 mW	80 mW	[35]
Photonic lantern	25/250	4.9 W	4.9 W	[36]
Photonic lantern	42/250	1007 W	219 W	This work

This has always been an extremely challenge in achieving high-power HOM output in LMA fiber lasers. As shown in Table 1, the previous work of other groups has been focused on mode-selective operation in fiber laser with core diameters below 25 μm. The previous work of our group only achieved near-FM output at the kilowatt level, but was not capable of controlling high-order modes [24]. Lu only achieved a 50-watt HOM output [26]. In this paper, for the first time, we have simultaneously realized a kilowatt-level FM and a hundred-watt-level HOM in 42-μm LMA fiber laser.

We observe that, despite the photonic lantern exhibits good mode control ability for LMA fiber amplifier, the beam quality of LP_{01} mode and the purity of LP_{11} mode appeared a certain degradation phenomenon with the increase of pump power. The decrease of beam quality and mode purity is primarily attributed to the transverse spatial-hole burning effect and the spatial mode competition in the LMA fiber amplifiers. In the next step, the implementation of specialty

https://doi.org/10.1017/hpl.2025.10059 Published online by Cambridge University Press

fibers, such as tapered fibers, could be strategically employed to mitigate the transverse spatial-hole burning effect and consequently enhance the mode purity[37, 38].

V. Conclusion

In this work, we demonstrate a kilowatt-level mode adaptive control of LMA fiber laser, the 5×1 photonic lantern is used as a mode converter to generate FM and HOMs respectively. Consequently, for LP_{01} mode control, a total of 1007 W output power with 18 GHz linewidth is obtained with the slope efficiency of 73%. We also achieve a stable LP_{11} mode output with an output power of 219 W and a high optical conversion efficiency of 75 %. The application of the few-ports photonic lantern in mode adaptive control of LMA fiber laser exhibit significant potential for high-power operation of specific mode in fiber lasers.

Acknowledgement

This work was supported by the National Natural Science Foundation of China (12074432).

References

1. A. Bouhelier, F. Ignatovich, A. Bruyant, C. Huang, G. C. d. Francs, J. C. Weeber, A. Dereux, G. P. Wiederrecht, and L. Novotny, "Surface plasmon interference excited by tightly focused laser beams," Optics Letters 32, 2535-2537 (2007).
2. P. Lebegue, J. De Sousa, C. Rapenau, D. Badarau, J. Andrieu, P. Audebert, F. Druon, and D. Papadopoulos, "Coherent combining of large-aperture high-energy Nd:glass laser amplifiers," High Power Laser Science and Engineering 13, e4 (2025).
3. T. Liu, S. Chen, X. Qi, and J. Hou, "High-power transverse-mode-switchable all-fiber picosecond MOPA," Optics Express 24, 27821-27827 (2016).
4. P. Ma, T. Yao, W. Liu, Z. Pan, Y. Chen, H. Yang, Z. Chen, Z. Wang, P. Zhou, and J. Chen, "A 7-kW narrow-linewidth fiber amplifier assisted by optimizing the refractive

https://doi.org/10.1017/hpl.2025.10059 Published online by Cambridge University Press

index of the large-mode-area active fiber," High Power Laser Science and Engineering 12, e67 (2024).

5. J. Ye, J. Xu, J. Song, Y. Zhang, H. Zhang, H. Xiao, J. Leng, and P. Zhou, "Pump scheme optimization of an incoherently pumped high-power random fiber laser," Photonics Research 7, 977-983 (2019).
6. Y. Zheng, Y. Yang, J. Wang, M. Hu, G. Liu, X. Zhao, X. Chen, K. Liu, C. Zhao, B. He, and J. Zhou, "10.8 kW spectral beam combination of eight all-fiber superfluorescent sources and their dispersion compensation," Optics Express 24, 2063-2071 (2016).
7. A. Kobyakov, M. Sauer, and D. Chowdhury, "Stimulated Brillouin scattering in optical fibers," Advances in Optics and Photonics 2, 1-59 (2010).
8. S. Ren, W. Lai, G. Wang, W. Li, J. Song, Y. Chen, P. Ma, W. Liu, and P. Zhou, "Experimental study on the impact of signal bandwidth on the transverse mode instability threshold of fiber amplifiers," Optics Express 30, 7845-7853 (2022).
9. M. A. Shevchenko, V. I. Grebenkin, M. V. Tareeva, A. D. Kudryavtseva, L. L. Chaikov, and N. V. Tcherniega, "Intracavity Stimulated Low-Frequency Raman Scattering," Bulletin of the Lebedev Physics Institute 45, 397-398 (2018).
10. L. Dong, "Accurate Modeling of Transverse Mode Instability in Fiber Amplifiers," Journal of Lightwave Technology 40, 4795-4803 (2022).
11. C. Jauregui, C. Stihler, and J. Limpert, "Transverse mode instability," Advances in Optics and Photonics 12, 429-484 (2020).
12. H. Li, J. Zang, S. Raghuraman, S. Chen, C. Goel, N. Xia, A. Ishaaya, and S. Yoo, "Large-mode-area multicore Yb-doped fiber for an efficient high power 976 nm laser," Optics Express 29, 21992-22000 (2021).
13. J. Song, S. Ren, G. Wang, H. Yang, Y. Chen, P. Ma, W. Liu, L. Huang, Z. Pan, and P. Zhou, "High Power Narrow-Linewidth Fiber Laser Based on Double-Tapered Fiber," Journal of Lightwave Technology 40, 5668-5672 (2022).
14. M. Chen, J. Cao, Q. Zhang, A. Liu, S. Zhou, Z. Huang, Z. Wang, and J. Chen, "Demonstration of hundred-watt-level near-diffraction-limited monolithic fiber laser near 980 nm with step-index double-cladding Yb-doped fiber," Optics Express 32, 13111-13118 (2024).

https://doi.org/10.1017/hpl.2025.10059 Published online by Cambridge University Press

15. B. Pulford, R. Holten, T. Matniyaz, M. T. Kalichevsky-Dong, T. W. Hawkins, and L. Dong, "kW-level monolithic single-mode narrow-linewidth all-solid photonic bandgap fiber amplifier," in *Conference on Fiber Lasers XIX ,(Technology and Systems at SPIE LASE Conference*, Proceedings of SPIE, 2022*)*, p.161-167.
16. Z. Xing, X. Wang, S. Lou, W. Zhang, S. Yan, and Z. Tang, "Bend-resistant side-leakage photonic crystal fiber with large-mode-area," Journal of Optics 21, 096731 (2019).
17. F. Anelli, A. Annunziato, A. M. Loconsole, S. Venck, S. Cozic, and F. Prudenzano, "Mode-Group Selective Photonic Lantern Based on Indium Fluoride Optical Fibers for Mid-Infrared," Journal of Lightwave Technology 43, 280-287 (2025).
18. D. Choudhury, D. K. McNicholl, A. Repetti, I. Gris-Sanchez, S. Li, D. B. Phillips, G. Whyte, T. A. Birks, Y. Wiaux, and R. R. Thomson, "Computational optical imaging with a photonic lantern," Nature Communications 11, 5217 (2020).
19. Y. Ding, J. Li, S. Li, Y. Qin, Z. Zhang, X. Wang, Y. Guo, X. Meng, and H. Du, "Eight Modes Selective Elliptic-Core Photonic Lantern in MIMO-Free Mode Division Multiplexing Systems at S plus C plus L Bands," Journal of Lightwave Technology 41, 739-744 (2023).
20. S. G. Leon-Saval, A. Argyros, and J. Bland-Hawthorn, "Photonic lanterns," Nanophotonics 2, 429-440 (2013).
21. S. G. Leon-Saval and Ieee, "The Photonic Lantern," in *23rd Opto-Electronics and Communications Conference (OECC)*, Opto-Electronics and Communications Conference-OECC 2018).
22. J. Montoya, C. Hwang, D. Martz, C. Aleshire, T. Y. Fan, and D. J. Ripin, "Photonic lantern kW-class fiber amplifier," Optics Express 25, 27543-27550 (2017).
23. J. Montoya, C. Aleshire, C. Hwang, N. K. Fontaine, A. Velazquez-Benitez, D. H. Martz, T. Y. Fan, and D. Ripin, "Photonic lantern adaptive spatial mode control in LMA fiber amplifiers," Optics Express 24, 3405-3413 (2016).
24. Y. Ze, P. Liu, H. Zhang, Y. Hu, L. Ding, B. Yan, J. Zhang, Q. Zhou, and W. Liu, "Realizing a kilowatt-level fiber amplifier with a 42 μ m core diameter fiber for improved multi-mode performance towards single mode operation output through adaptive spatial mode control utilizing a 3x1 photonic lantern," Optics Express 32, 35794-35805 (2024).

https://doi.org/10.1017/hpl.2025.10059 Published online by Cambridge University Press

25. Y. Lu, Z. Chen, W. Liu, M. Jiang, J. Yang, Q. Zhou, J. Zhang, J. Chai, and Z. Jiang, "Stable single transverse mode excitation in 50 μm core fiber using a photonic-lantern-based adaptive control system," Optics Express 30, 22435-22441 (2022).
26. Y. Lu, Z. Jiang, Z. Chen, M. Jiang, J. Yang, Q. Zhou, J. Zhang, D. Zhang, J. Chai, H. Yang, and W. Liu, "High-Power Orbital Angular Momentum Beam Generation Using Adaptive Control System Based on Mode Selective Photonic Lantern," Journal of Lightwave Technology 41, 5607-5613 (2023).
27. Y. Lu, Z. Jiang, H. Xiao, Z. Chen, M. Jiang, J. Chai, H. Yang, L. Ding, D. Zhang, J. Zhang, Q. Zhou, and W. Liu, "Mitigating mode instabilities by controllable mode beating excitation with a photonic lantern," Frontiers in Physics 11, 1198092 (2023).
28. Y. Wen, P. Wang, B. Yang, H. Zhang, X. Xi, X. Wang, and X. Xu, "First Demonstration and Comparison of 5 kW Monolithic Fiber Laser Oscillator Pumped by 915 nm and 981 nm LDs," Photonics 9, 716 (2022).
29. Y. Ze, P. Liu, H. Zhang, Y. Hu, L. Ding, B. Yan, J. Zhang, Q. Zhou, and W. Liu, "The Simulation of Mode Control for a Photonic Lantern Adaptive Amplifier," Micromachines 15, 1342 (2024).
30. H. Wang, M.-Y. Chen, Y.-F. Zhu, S.-Y. Li, P. Yin, X.-S. Wu, R.-H. Li, Z.-M. Cai, P.-P. Fu, H. Qin, and J. Wei, "Design and demonstration of single-mode operation in few-mode optical fiber with low-bending loss," Optical Engineering 56, 016103 (2017).
31. O. Shapira, A. F. Abouraddy, J. D. Joannopoulos, Y. Fink, and Ieee, "Complete modal decomposition for optical waveguides," in *Conference on Lasers and Electro-Optics (CLEO)*, 2005), pp.1551-1553.
32. X. Yang, Z.-H. Xu, S.-P. Chen, and Z.-F. Jiang, "High power LP₁₁ mode supercontinuum generation from an all-fiber MOPA," Optics Express 26, 13740-13745 (2018).
33. R. Su, B. Yang, X. Xi, P. Zhou, X. Wang, Y. Ma, X. Xu, and J. Chen, "500 W level MOPA laser with switchable output modes based on active control," Optics Express 25, 23275-23281 (2017).
34. Y. You, G. Bai, X. Zou, X. Li, M. Su, H. Wang, Z. Quan, M. Liu, J. Zhang, Q. Li, H. Shen, Y. Qi, B. He, and J. Zhou, "A 1.4-kW Mode-Controllable Fiber Laser System," Journal of Lightwave Technology 39, 2536-2541 (2021).

https://doi.org/10.1017/hpl.2025.10059 Published online by Cambridge University Press

35. N. Wang, J. C. A. Zacarias, J. E. Antonio-Lopez, Z. S. Eznaveh, C. Gonnet, P. Sillard, S. Leon-Saval, A. Schulzgen, G. Li, and R. Amezcua-Correa, "Transverse mode-switchable fiber laser based on a photonic lantern," Optics Express 26, 32777-32787 (2018).
36. S. Wittek, R. B. Ramirez, J. A. Zacarias, Z. S. Eznaveh, J. Bradford, G. L. Galmiche, D. Zhang, W. Zhu, J. Antonio-Lopez, L. Shah, and R. A. Correa, "Mode-selective amplification in a large mode area Yb-doped fiber using a photonic lantern," Optics Letters 41, 2157-2160 (2016).
37. A. P. Napartovich and D. V. Vysotsky, "Theory of spatial mode competition in a fiber amplifier," Physical Review A 76, 063801 (2007).
38. Z. Jiang and J. R. Marciante, "Impact of transverse spatial-hole burning on beam quality in large-mode-area Yb-doped fibers," Journal of the Optical Society of America B-Optical Physics 25, 247-254 (2008).

https://doi.org/10.1017/hpl.2025.10059 Published online by Cambridge University Press